Energetics of lithium ion adsorption on defective carbon nanotubes

Kazume Nishidate* and Masayuki Hasegawa
Faculty of Engineering, Iwate University, Morioka 020-8551, Japan
(Received 11 January 2005; revised manuscript received 5 April 2005; published 30 June 2005)

We apply the density-functional theory to study energetics of lithium ion adsorption on single-wall carbon nanotubes (SWNTs). We use both the local-density approximation (LDA) and the generalized-gradient approximation (GGA) for the exchange-correlation energy functional. Both the LDA and GGA calculations indicate that adsorption processes of lithium onto the pristine and defective (8,0) SWNT are exothermic with respect to the metallic lithium. On the other hand, the lithium adsorption on the (5,5) SWNT can be endothermic depending on the defect structures. As the defective ring on the surface becomes large, the energy barrier for lithium diffusion through the ring lowers and the peak position of the barrier shifts toward the center of the SWNT. Molecular dynamics simulations are also performed to study the diffusion dynamics of the lithium into the SWNT through the defective rings on the sidewall. These results suggest the possibility of accumulating lithium ions inside the SWNT with large defective rings.

DOI: 10.1103/PhysRevB.71.245418 PACS number(s): 61.46.+w, 71.15.Mb, 71.15.Pd, 71.20.Tx

I. INTRODUCTION

Rechargeable lithium ion batteries have been widely used as the compact power sources for information technology devices. The charging and discharging process in these batteries is controlled by exchanging lithium ions between the negative and positive electrodes through the separator.[1] The desired features of electrode materials are (i) large electronic capacity, (ii) good reversibility, (iii) quick charging process, and (iv) environment-friendly characteristics, while serving the economical issues. Although lithium in the metallic state is favorable as a negative electrode to achieve maximal performance, it is not suitable for practical use because of its explosive nature.

The lithium-graphite intercalation compound (Li-GIC) has been extensively studied[2,3] and widely used as the negative electrode in the commercial lithium ion rechargeable batteries.[1] Recently, it has been suggested, both experimentally and theoretically, that the carbon nanotube is one of the most promising candidates to replace the Li-GIC negative electrode. Zhao *et al.*[4] investigated the possibility of achieving the lithium capacity of the nanotubes corresponding to the stoichiometry of LiC_2, which is considerably improved compared to the Li-GIC (LiC_6). The long pristine nanotubes, however, are not suitable for the electrode since its interior can hardly be used for the lithium adsorption. Experimentally, lithium capacity of the nanotube can be significantly increased up to the stoichiometry of LiC_3 by ball milling nanotubes into the fractured structure or chemically etching them to the short segments. Lithium could easily diffuse not only to the exterior but also to the interior through the created defects or the open ends of such nanotubes.[5,6] Meunier *et al.*[7] studied lithium diffusion into the (5,5) and (8,0) carbon nanotubes through the created defective rings by *ab initio* calculations based on the density-functional theory (DFT). They estimated the diffusion-barrier and defect-formation energies for the topological defects of the (5,5) nanotube, but detailed analyses were not made for the lithium adsorption energies.

In the present work we investigate the detailed energetics of lithium ion adsorption on the defective single-wall carbon nanotubes (SWNTs) by the DFT total-energy calculations. We use both the local-density approximation (LDA)[8,9] and the generalized-gradient approximation (GGA:PW91)[10] for the exchange-correlation energy functional to examine the lithium adsorption performance of SWNT with defect. The dynamics of lithium diffusion through the defective SWNT is studied by using the first-principles molecular dynamics (MD) simulation method, in which all the atoms are allowed to move following the Newtonian equation of motion, while the electronic states are solved exactly at each time step.

II. DEFECT FORMATION ENERGY

The total energy calculations were performed using the first-principles simulation code VASP[11,12] and the spin-polarized projector augmented-wave (PAW) method[13,14] was also used. Well-converged cutoff energy of 300 eV was used in the plane-wave expansion, and only the Γ point was considered in the reciprocal space integration. We used a large rectangular supercell to simulate the isolated defective SWNT in the vacuum. Two types of SWNTs, metallic (5,5) armchair and semiconducting (8,0) zigzag, were chosen as samples in our calculations since the diameters of these SWNTs are nearly the same. The diameters of the (5,5) and (8,0) SWNTs are 6.78 and 6.26 Å, respectively. The size of the supercell in the radial direction was taken to be 20×20 Å^2 and the length in the axial direction was taken to contain six and four units of SWNTs, being equal to 14.76 and 17.04 Å, for the (5,5) and (8,0) SWNTs, respectively. We used the experimental carbon-carbon bond length of graphite (1.42 Å) to construct the SWNT, and the atomic coordinates were fully relaxed using the conjugate gradient algorithm with a tolerance of 0.05 eV/Å for maximal atomic force.

We calculate the formation energies of n-membered topological ring defects with $n=7$ (heptagon), $n=8$ (octagon), and $n=9$ (enneagon). Since the number of atoms of each defective system is the same as that of the corresponding

TABLE I. Defect formation energies E_f^n (in electron volts) of n membered carbon rings for (5,5) and (8,0) SWNTs calculated in the LDA and GGA and their comparisons to the LDA results obtained by Meunier *et al.* (Ref. 7).

	(5,5)			(8,0)		
	$n=7$	$n=8$	$n=9$	$n=7$	$n=8$	$n=9$
LDA	3.90	7.09	10.07	2.81	5.92	8.94
GGA	4.23	7.60	9.66	2.36	5.73	8.79
LDA[a]	3.5	6.2	9.5			

[a]Reference 7.

pristine SWNT, defect formation energy E_f^n of n-membered rings can be simply evaluated by comparing the total energy of defective SWNT (E_{tot}^n) with that of the pristine SWNT (E_{tot}),

$$E_f^n = E_{\text{tot}}^n - E_{\text{tot}}. \quad (1)$$

Although the orientation of the defective ring on the SWNT surface is optional to some extent, we consider only the energetically most favorable configurations determined by the total energy calculations. The results of E_f^n are summarized in Table I. The defect formation energy increases with the number n in accordance with the expectation. The formation energies calculated in the LDA are higher than the those in the GGA except for the $n=7$ and $n=8$ rings of the (5,5) SWNT. Calculated LDA values of E_f^n of a graphene sheet,[15] which can be regarded as a SWNT in the limit of large diameter, are 4.92 eV ($n=7$), 10.53 eV ($n=8$), and 15.86 eV ($n=9$). These values are significantly higher than those of the SWNTs, indicating that SWNTs are more fragile than the graphene sheet against the defect formation. Our LDA values of E_f^n for (5,5) SWNT are larger by ~0.5 eV than the previous calculations by Meunier *et al.*[7] Although we cannot trace this discrepancy because they did not provide computational details, such as the supercell size, it may be caused by the numerical inaccuracies originating from their use of the norm-conserving pseudopotential, which requires substantially larger cutoff energies than the PAW to achieve the same accuracy in the plane-wave expansion.[14]

The structures of the defective SWNTs obtained by the GGA are shown in Fig. 1. The defective rings are shifted to the interior of SWNTs to conserve the carbons-carbon bond length (r_{cc}) of the rings. In general, distortion spreads to a larger extent over the SWNT as the number n increases and the strong three-dimensional deformation for the $n=9$ ring is noticeable. We also find that the stress induced by the $n=8$ ring of the (8,0) SWNT is effectively released by the distorted expansion of the SWNT in contrast to the case of $n=8$ ring of the (5,5) SWNT where the stress is released mostly by the radial shrink of the SWNT.

The mean bond length (r_{cc}) of the carbons making up the n-membered ring are presented in Table II. It is known that the LDA usually underestimates the bond length, whereas the GGA tends to overestimate it. This feature is also found in the present results, but the quantitative differences between

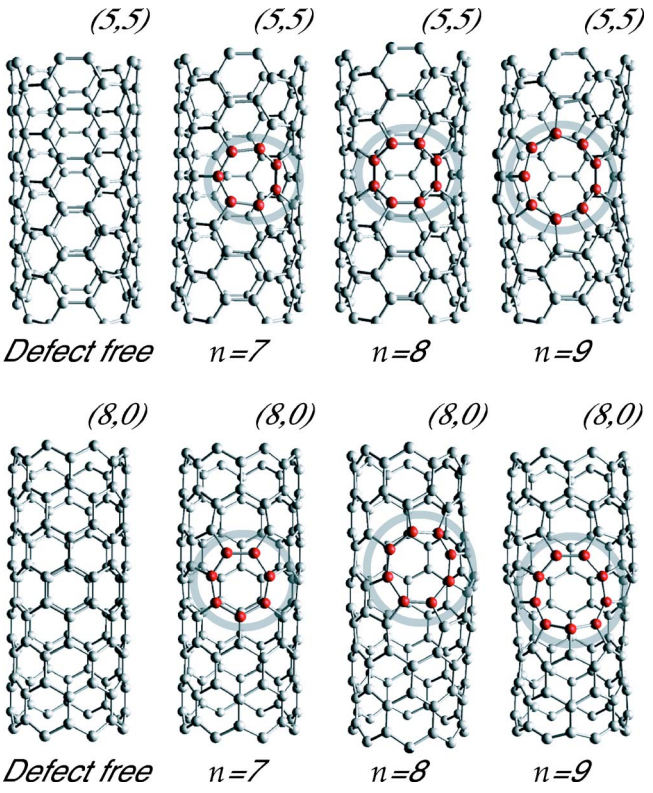

FIG. 1. (Color online) Fully relaxed structures of the defect-free and the defective (5,5) (upper panel) and (8,0) (lower panel) SWNTs obtained by the GGA calculations. Gray balls and rods are the carbon atoms and bonds shorter than 1.5 Å, respectively. Carbon ring defects are indicated by the thick circles. The structures obtained by the LDA calculations are indistinguishable from the GGA results on this scale.

both results are very small and <0.02 Å. We see that the calculated mean r_{cc} for the $n=7$ and $n=8$ rings of the (5,5) SWNT are shorter than that of the graphene (1.42 Å). In contrast to this, those for the defective rings of the (8,0) SWNT are longer than that of the graphene, indicating that the stress induced by the defective rings of the (8,0) SWNT is effectively released by extending the bond lengths. These results for the defective ring on the (8,0) SWNT may be the consequence of the geometrical feature and expected to be found in the other defective rings on a similar $(n,0)$, zigzag SWNT (n:integer) with small diameter. For the ring defects with shorter r_{cc} [$n=7$ and $n=8$ rings of the (5,5) SWNT] than that of the defect-free system, the defect formation energies

TABLE II. Mean bond length (in angstroms) of the carbons making up the n-membered rings for (5,5) and (8,0) SWNTs obtained after the structural relaxations.

	(5,5)				(8,0)			
	Defect free	$n=7$	$n=8$	$n=9$	Defect free	$n=7$	$n=8$	$n=9$
LDA	1.420	1.404	1.388	1.439	1.427	1.452	1.444	1.438
GGA	1.427	1.413	1.396	1.447	1.433	1.460	1.453	1.456

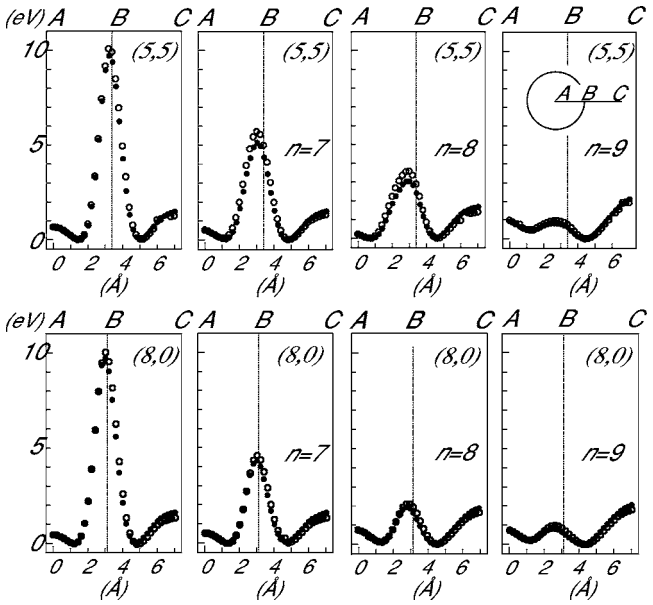

FIG. 2. Energetics of diffusion pathways for lithium to move through the center of the n rings of the (5,5) and (8,0) SWNTs. The result for the defect-free (pristine) SWNT is given in the left end for each case. The energy zero is taken to be that of the most stable point. Solid (open) circles are the results of the LDA (GGA) calculations. A, B, and C represent the spatial points where lithium is on the axis, on the surface (center of the ring), and in exterior of the SWNT, respectively, as schematically shown in the inset of the upper-right graph. The scale of the horizontal axis is the distance (in angstroms) from the central axis (point A). The vertical dotted line is the SWNT surface (point B), formally defined as half of the diameter.

calculated in the GGA are higher than those of the LDA by 0.3–0.5 eV, implying the tendency of the GGA to yield larger strain energy due to the defective ring formation.

III. ENERGETICS OF LITHIUM DIFFUSION PATHWAYS

The global energy minimum is achieved when lithium is on top of the center of the ring formed by carbon atoms. We therefore investigated the energetics of diffusion pathways for lithium to move through the center of defective rings. The results are shown in Fig. 2. In these calculations, the atomic structures of the SWNTs are frozen in their equilibrium configurations obtained in the absence of lithium and each electronic state of the SWNTs with lithium is solved to be in the ground state. The calculated total energies show smooth variation along the diffusion pathways, indicating relative accuracy of the calculations. The energy barrier for the lithium diffusion is defined as the energy difference between the configurations in which the lithium is placed at the most stable and the most unstable positions on the diffusion pathway, which can be obtained as the peak heights in Fig. 2 and are presented in the Table III. The energy barrier for the hexagonal ring (defect-free case) amounts to about 10 eV, which is about 4 eV lower than the LDA result obtained by Meunier *et al.*[7] but still too high for the inenergetic lithium to get through the ring. As the defective ring becomes large, the energy barrier lowers and its peak position shifts toward the center of the SWNT, which corresponds to the shift of the defective ring to the interior. For the $n=9$ defective ring, the energies at the stable point in the interior are 0.5 and 0.22 eV higher than that in the exterior for the (5,5) and (8,0) SWNTs, respectively. The energy barriers for the $n=7$ and $n=8$ rings of the (5,5) SWNT are about 1 eV higher than those of the (8,0) SWNT. This can be understood from the fact that r_{cc} of the $n=7$ and $n=8$ rings of the (5,5) SWNT are shorter than that of the graphene (1.42 Å). Here, the energy barrier calculated by the LDA for the $n=9$ defective ring of a graphene is only 0.62 eV,[15] which is about 0.2 eV lower than the corresponding value of the (8,0) SWNT.

TABLE III. Energy barrier (in electron volts) for the lithium diffusion through the center of the rings obtained by the LDA and GGA calculations. The LDA results obtained by Meunier *et al.* (Ref. 7) are also presented for comparison.

	(5,5)				(8,0)			
	Defect free	$n=7$	$n=8$	$n=9$	Defect free	$n=7$	$n=8$	$n=9$
LDA	9.70	5.15	3.02	0.84	9.70	4.28	1.92	0.81
GGA	10.12	5.72	3.58	0.96	10.07	4.59	2.12	1.00
LDA[a]	13.5	7.5	3.0	0.5				

[a]Reference 7.

The distances, measured along the diffusion pathways, between the most stable point and the center of the defective ring for the (5,5) and the (8,0) SWNTs are summarized in the Table IV. In the cases where the lithium is adsorbed to the

TABLE IV. Distances (in angstroms) between the stable positions for lithium and the center of the defective n ring of the (5,5) and (8,0) SWNTs obtained by the LDA and GGA calculations. The *interior* and *exterior* indicate that lithium is adsorbed on the interior and exterior sides of the SWNT, respectively.

		Interior				Exterior			
		Defect free	$n=7$	$n=8$	$n=9$	Defect free	$n=7$	$n=8$	$n=9$
(5,5)	LDA	1.91	2.30	2.65	2.14	1.65	1.40	1.16	0.98
	GGA	1.95	2.36	2.75	2.18	1.72	1.51	1.28	1.11
(8,0)	LDA	1.93	1.80	2.00	1.92	1.64	1.58	1.16	1.04
	GGA	1.96	1.83	2.01	1.97	1.75	1.62	1.30	1.19

TABLE V. Lithium adsorption energy ΔE (in electron volts) for the (5,5) and (8,0) SWNTs obtained by the LDA and GGA calculations. The *interior* and *exterior* are the same as in Table IV. The positive (negative) value indicates that the reaction is endothermic (exothermic) with respect to the metallic lithium.

		Interior				Exterior			
		Defect free	$n=7$	$n=8$	$n=9$	Defect free	$n=7$	$n=8$	$n=9$
(5,5)	LDA	0.52	0.46	0.15	−0.20	0.57	0.42	0.20	−0.63
	GGA	0.05	0.24	−0.07	−0.45	0.06	0.28	−0.07	−0.95
(8,0)	LDA	−0.38	−0.34	−0.68	−0.77	−0.35	−0.27	−0.73	−0.94
	GGA	−0.11	−0.08	−0.42	−0.50	−0.13	−0.04	−0.52	−0.71

exterior of the SWNT, the distances between the stable lithium positions and the defective rings decrease as the number n increases. We note that these distances for the (5,5) SWNT are shorter than those for the defect-free case, which is a consequence of the structural deformation characteristic of the (5,5) SWNT.

For these stable lithium positions we evaluated lithium adsorption energy ΔE defined by

$$\Delta E = E^n_{\mathrm{SWNT+Li}} - E^n_{\mathrm{SWNT}} - \mu_{\mathrm{Li(bcc)}}, \tag{2}$$

where $E^n_{\mathrm{SWNT+Li}}$ and E^n_{SWNT} are the total energies of the SWNT with the n ring in the presence and absence of the adsorbed lithium, respectively, and $\mu_{\mathrm{Li(bcc)}}$ is the atomic chemical potential of the metallic lithium with the bcc structure, which is experimentally known to be the most stable phase under normal conditions.[16,17] We relaxed the bcc structure of the lithium and calculated the total energies in the LDA and GGA. We used the cutoff energy of 147 eV in the plane-wave expansion, and reciprocal space integrations were performed using $20^3$$k$-point mesh.[18] The optimized lattice constants are 3.35 Å (LDA) and 3.44 Å (GGA), which are compared to the experimental value of 3.49 Å at 78 K.[16]

The lithium adsorption energies calculated in this way for the (5,5) and (8,0) SWNTs are summarized in the Table V. Here we note that the $E^n_{\mathrm{SWNT+Li}}$ is defined as the minimum value of the energy curve shown in Fig. 2 and ΔE is the adsorption energy in the sense that the lithium is captured *near* the defective ring. The adsorption energy when lithium is captured by the SWNT far from the defective ring can be obtained by calculating ΔE for the defect-free SWNT, which are also given in Table V. The LDA results for ΔE show that the adsorption of lithium onto the $n=7$ and $n=8$ defective rings and the defect-free hexagonal ring of the (5,5) SWNT are endothermic reactions with respect to the metallic lithium. On the other hand, both the LDA and GGA predict that the lithium adsorption onto the (8,0) SWNT are exothermic. In the latter case adsorption energies calculated in the LDA are lower than those in the GGA in contrast to the case of (5,5) SWNT, where GGA gives lower adsorption energies. In our calculations, the adsorbed lithium atoms are almost completely ionized to be monovalent by transferring the 2s valence electron to the SWNTs, as reported previously.[5–7]

At the initial stage of charging process, monovalent lithium ions on the positive electrode move to the negative electrode through the separator in the battery cell. On the other hand, electrons released from the lithium ions on the positive electrode are forced to move through an external circuit driven by the supplied electric power and are stored at the negative electrode with the adsorbed monovalent lithium ions. Therefore the balance of the total energies at the positive and negative electrodes, with or without lithium ions, directly correlates with the expected average voltage and this enables us to estimate the averaged power of the battery cell from the total energy calculations.[19,20] The average voltage V_{av} is given by

$$V_{\mathrm{av}} = -\frac{\Delta G}{F}, \tag{3}$$

where F is the Faraday constant and ΔG is the change in the Gibbs free energy in the discharge reaction at the positive electrode composed of a transition metal oxide (TMO),

$$x\mathrm{Li} + \mathrm{TMO} \rightarrow \mathrm{Li_x TMO}. \tag{4}$$

Since the changes in the volume and entropy have limited effects on ΔG, it can be approximated by the change in the internal energy obtained from the total energy calculations. It has been reported that the typical values of V_{av} for the cathode composed of TMO (e.g., manganese oxide) evaluated in this way amount to 3–4 V.[19,20] We can also expect the change in the Gibbs free energy $\Delta G'$ in the discharge reaction at the negative electrode composed of the SWNTs,

$$\mathrm{Li}_x\mathrm{@SWNT} \rightarrow x\mathrm{Li} + \mathrm{SWNT}, \tag{5}$$

where $\Delta G'$ can be approximated by the lithium *desorption* energy ($\approx -\Delta E$). When every hexagonal ring of the SWNT captures one lithium atom the stoichiometry becomes LiC_2, which corresponds to the estimated upper limit of the lithium capacity of SWNT. By neglecting the scattering of adsorption energies given in Table V and interactions between lithium ions, the change in the total energy per LiC_2 can be roughly estimated to be $|\Delta E_{\mathrm{LiC_2}}| = 0.5$ eV at most. This can be understood because the net number of carbon atoms belonging to a hexagonal ring is two (more for the defective rings) and the amount of the lithium adsorption energy for a ring on the SWNT is typically $|\Delta E| \leqslant 0.5$ eV (Table V). Then the change in the total average voltage caused by the lithium adsorption on every possible site of the defective SWNT anode can be rudely estimated to be $|\delta V'_{\mathrm{av}}| \leqslant |\Delta E_{\mathrm{LiC_2}}/F| \approx 0.5$ V. This result for the stoichiometry of LiC_2 suggests that $|\delta V'_{\mathrm{av}}|$ at the experimental stoichiometry limit of LiC_3 is

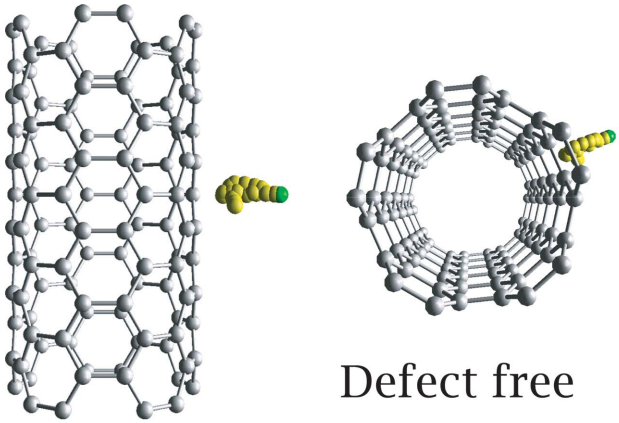

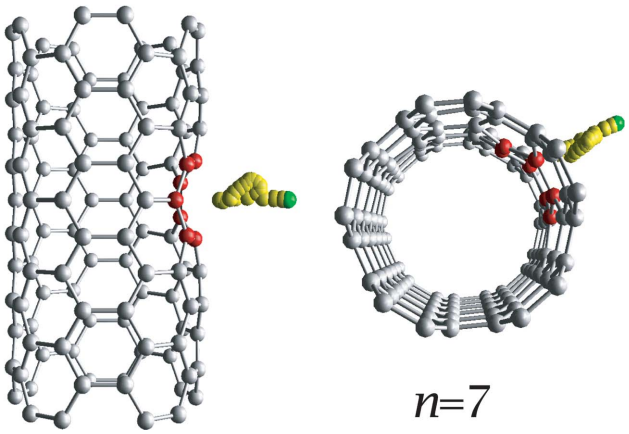

FIG. 3. (Color) Snap shots of the lithium diffusion to the defect-free hexagonal ring (upper panel) and to the $n=7$ defective ring (lower panel) of the (5,5) SWNT. The side (left panel) and the top (right panel) views are presented. The initial structure of the SWNT (gray balls and the framework) is superimposed for the eye's guide. The atoms making up the defective ring are indicated by the red balls. The total number of MD time steps is 125 (250 fs) and only the lithium trajectory for every five MD steps are shown (yellow balls). The initial position of the lithium is indicated by the green balls.

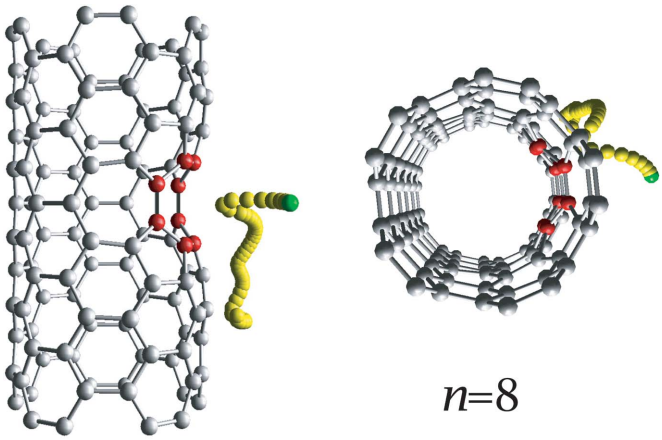

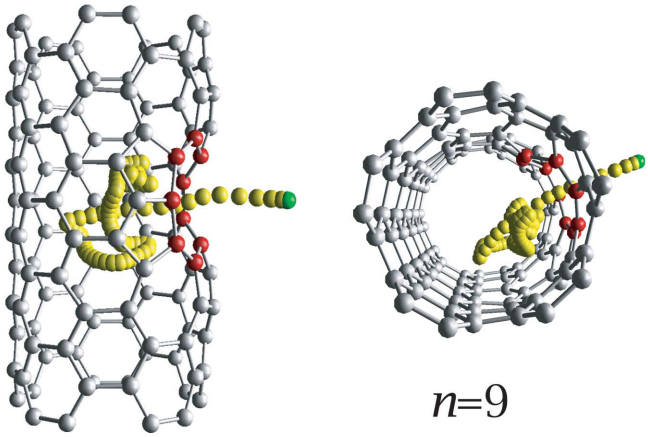

FIG. 4. (Color) Snap shots of the lithium diffusion to the $n=8$ defective ring (upper panel) and to the $n=9$ defective ring (lower panel) of the (5,5) SWNT. The other details are the same as those in Fig. 3 except that the total number of MD time steps is 525 (1050 fs) for the $n=9$ case. The acceleration of the lithium motion on approaching the $n=9$ defective ring is clearly seen from the trajectory.

two-thirds of that for LiC_2 (i.e., $|\delta V'_{av}| \leq 0.3V$). Hence the SWNTs with lithium ions adsorbed on both the exterior and interior sides could behave as a stable anode comparable to the lithium metal anode.

IV. MOLECULAR DYNAMICS OF LITHIUM DIFFUSION

To investigate the dynamics of the lithium ion diffusion through the defective rings of the (5,5) SWNT, we performed molecular dynamics (MD) simulations. We used the cutoff energy of 300 eV in the plane-wave expansion and only the Γ point is considered in the reciprocal space integrations. The supercell used in these calculations is the same as that described earlier. All the atomic motions are updated by the predictor-corrector method, whereas the electronic states are maintained in their instantaneous ground states at each MD time step with the increment $\Delta t=2$ fs. A Maxwell-Boltzmann-type velocity distribution corresponding to 1000 K is assumed as the initial condition, and temperature is not controlled afterward (NVE ensemble). The initial temperature descended rapidly to the steady value about 535 K and, at the same time, the total energies were stabilized. Temperature-controlled MD simulations at 300 K using the Nosé thermostat method[21] gave essentially the same results.

Initially the lithium atom is placed outside the SWNT, right above the center of the ring, at the position 3.22 Å from the sidewall (slightly outside the stable position), and no external force is applied. Since this initial position corresponds to the hillside of the potential as shown in Fig. 2, the lithium atom spontaneously moves toward the center of the ring. Trajectories of the lithium ion diffusion to the defect-free hexagonal ring and the defective rings ($n=7$, $n=8$, and $n=9$) are illustrated in Figs. 3 and 4. The lithium ion cannot get through the defect-free hexagonal ring because of the high energy barrier of ~ 10 eV but is driven back and then drifting about the stable position outside the ring. Similar behavior is found for the lithium ion diffusion to the $n=7$

ring. In the case of the $n=8$ ring, the lithium ion approaches the ring at first stages, but it is then turned back and starts to move over the external surface. In contrast, the lithium ion can diffuse into the SWNT through the $n=9$ defective ring and we can see the acceleration of the lithium ion motion on approaching the ring (Fig. 4). The lithium ion captured inside the SWNT then starts to move about in the interior, and its desorption is rarely allowed afterward. The energy barrier is low but contributes to accumulating lithium ions inside the SWNTs during the charging process.

V. SUMMARY

We confirmed that the defect formation energy of SWNTs increases as the defective ring becomes large. The energy barrier for the lithium diffusion lowers with increasing size of the defective ring. Also, the peak position of the energy barrier along the diffusion pathway shifts toward the center of the SWNT as the size of the defective ring becomes large. The stable positions for the lithium inside the SWNTs with $n=8$ defective ring shift to the inner sides, which is required to moderately conserve the r_{cc} of the ring. Although no significant difference is found between the relaxed structures calculated in the LDA and GGA, different results are obtained for the lithium adsorption energies. Both the LDA and GGA predict that adsorption processes of lithium onto the pristine and defective (8,0) SWNT are exothermic, whereas adsorption of the lithium to the (5,5) SWNT can be endothermic in some cases depending on the approximations used for the exchange-correlation functionals.

Molecular-dynamics calculations showed that the lithium cannot diffuse through the defect-free hexagonal ring and the $n=7$ and $n=8$ defective rings of the (5,5) SWNT but can diffuse into the (5,5) SWNT through the $n=9$ defective ring. The lithium captured inside the SWNT then moves about in the interior, and successive adsorption of lithium through the defective ring could be allowed, indicating the possibility of accumulating lithium atoms inside the SWNT.

ACKNOWLEDGMENTS

This work was supported by a Grant-in-Aid for Scientific Research from the Ministry of Education, Culture, Sports, Science and Technology through Grants No. 16550002 and No. 16540301. The computations in the present work were performed using the facilities of the Supercomputer Center, Institute for Solid State Physics, University of Tokyo, and the Information Processing Center of Iwate University. We thank Y. Sakai, Y. Nihe, Y. Matsukura, K. Ohta, and H. Ojima for assistance in the computations.

*Electronic address: nisidate@iwate-u.ac.jp

[1] M. Winter, J. Besenhard, M. Spahr, and P. Nóvak, Adv. Mater. (Weinheim, Ger.) **10**, 725 (1998).
[2] K. R. Kganyago and P. E. Ngoepe, Phys. Rev. B **68**, 205111 (2003).
[3] M. Khantha, N. A. Cordero, L. M. Molina, J. A. Alonso, and L. A. Girifalco, Phys. Rev. B **70**, 125422 (2004).
[4] J. Zhao, A. Buldum, J. Han, and J. Lu, Phys. Rev. Lett. **85**, 1706 (2000).
[5] B. Gao, C. Bower, J. Lorentzen, L. Fleming, A. Kleinhammes, X. Tang, L. McNeil, Y. Wu, and O. Zhou, Chem. Phys. Lett. **327**, 69 (2000).
[6] H. Shimoda, B. Gao, X. P. Tang, A. Kleinhammes, L. Fleming, Y. Wu, and O. Zhou, Phys. Rev. Lett. **88**, 015502 (2001).
[7] V. Meunier, J. Kephart, C. Roland, and J. Bernholc, Phys. Rev. Lett. **88**, 075506 (2002).
[8] D. M. Ceperley and B. J. Alder, Phys. Rev. Lett. **45**, 566 (1980).
[9] J. P. Perdew and A. Zunger, Phys. Rev. B **23**, 5048 (1981).
[10] J. P. Perdew and Y. Wang, Phys. Rev. B **45**, 13244 (1992).
[11] G. Kresse and J. Hafner, Phys. Rev. B **47**, R558 (1993).
[12] G. Kresse and J. Furthmüller, Phys. Rev. B **54**, 11169 (1996).
[13] P. E. Blöchl, Phys. Rev. B **50**, 17953 (1994).
[14] G. Kresse and D. Joubert, Phys. Rev. B **59**, 1758 (1999).
[15] In the calculations for the hexagonal graphene sheet we used a large supercell containing 6×6 unit cells in the plane and with the virtical size of 6.0 Å. Only the Γ point was used for the reciprocal space integrations, and a cutoff energy of 400 eV was used in the plane-wave expansion.
[16] N. Ashcroft and N. Mermin, *Solid State Physics* (Saunders College Publishing, New York, 1976), p. 70.
[17] M. Winter, *WebElements Periodic Table*, (WebElements, Sheffield UK, 2004), http://www.webelements.com/
[18] H. J. Monkhorst and J. D. Pack, Phys. Rev. B **13**, 5188 (1976).
[19] M. K. Aydinol, A. F. Kohan, G. Ceder, K. Cho, and J. Joannopoulos, Phys. Rev. B **56**, 1354 (1997).
[20] S. K. Mishra and G. Ceder, Phys. Rev. B **59**, 6120 (1999).
[21] S. Nosé, J. Chem. Phys. **81**, 511 (1984).